Raja Bala and Gaurav Sharma

System Optimization in Digital Color Imaging

Understanding and exploiting interactions

For reasons of tractability and modular design, it is common practice to partition digital color imaging systems into components based on the functionality they provide. Examples of these components include image segmentation, enhancement, compression, color characterization, and halftoning. Many of these topics are described in detail in other articles in this issue. Typically, the components are individually designed and optimized, and the partitioning has the unintended consequence that engineers working on specific components acquire expertise limited to those components and think "within the box" for solving problems they encounter. This article highlights the system interactions among these components and illustrates, through a series of examples, how knowledge of system interactions may be beneficially exploited to improve color quality and/or performance of the end-to-end system. Examples are specifically chosen to highlight concepts in color image processing, and a set of illustrative images is included with the examples. In our presentation, we assume that the reader is familiar with the basics of color imaging and device characterization. The introductory article of this issue [1] provides a brief primer, and additional background material can be found in [2].

The following presents an overview of a color imaging system and its elements and then highlights techniques in the literature that attempt to account for system interactions for improved quality or performance. After that, presented in greater detail, are two specific examples of approaches that take into account interactions between elements that are normally treated independently. Finally, concluding remarks are presented.

COLOR IMAGING SYSTEM ELEMENTS

The diagram of Figure 1 illustrates the components that are commonly identified as the building blocks of an end-to-end digital color imaging system. A more detailed example illustrating

1053-5888/05/$20.00©2005IEEE

the elements of a digital camera, which is a specific input digital imaging system, may be found in a companion article in this issue [3] and in [4]. The chain typically begins with analog images that exist as real world scenes or as hardcopy images on a physical medium. Image capture devices, such as scanners and digital cameras, are used to capture and digitize these analog images. The capture step is followed by digital image processing elements that perform input related processing tasks. For digital color cameras, such tasks include demosaicking [5], [6], white balance correction for the illumination under which the image is captured, and input color management to correct for the camera color characteristics [7]. For scanners, the processing involves correction of optical artifacts, such as integrating cavity effect [8], descreening for halftoned input [9]–[11], segmentation of the scanned image into regions corresponding to text, graphics, and pictorials, and color management to correct for the scanner's color response [7]. The next step in the imaging chain normally consists of processing for the purpose of image archival, exchange, and transmission and includes steps such as transformation to standard color spaces, dynamic range reduction [12], quantization, and compression [13]. For synthetic computer generated imagery, these are typically the first processing steps. On the output side of the digital color imaging chain, the digital output processing includes steps preliminary to output rendition; primary among these are color characterization for the output device [7], gamut mapping [12], color quantization for palettized displays [14], and halftoning [15]. The final step on the output side consists of image rendition on a printer or a display and produces, as an end result, an image on a physical medium. The human visual system (HVS) is typically the end consumer of imagery generated from the system, and in some scenarios, may be involved in comparing the original (or recollection thereof) with the output from the system. Characteristics of the HVS are therefore commonly exploited throughout the imaging system. Note that this end-to-end representation of an imaging system is intended for conceptual understanding and for illustration of the interrelations among the individual elements. In practical systems, a single device may encapsulate a number of elements, including some that are not necessarily sequential, and not all the elements that are discussed here may be present in every imaging system. The design of digital color imaging systems incorporates some understanding of the overall system elements and their interactions. In particular, for imagery intended for a human observer, the characteristics of the HVS influence the design of several of the components; specific examples being the compression and halftoning operations that exploit the low-pass characteristics of the HVS. Particular examples related to color processing are the use of luminance-chrominance (e.g., YIQ) encodings for image compression with significantly smaller bandwidths for the chrominance channel in comparison to the luminance; the use of device independent color description for decoupling input and output color devices [16], and a power-law nonlinearity for encoding color values. However, once the individual elements have been defined, they are often optimized individually without regard to the interplay among the components. It is our goal in this article to illustrate that a system-wide understanding can often be exploited further when considering several of the elements, either jointly or individually, to better exploit cost, performance, and quality tradeoffs in digital imaging systems. We believe these system

A PRIMARY GOAL OF COLOR MANAGEMENT IN HARDCOPY IMAGING SYSTEMS IS TO ACHIEVE CONSISTENT AND ACCURATE COLOR REPRODUCTION ACROSS DIFFERENT DEVICES.

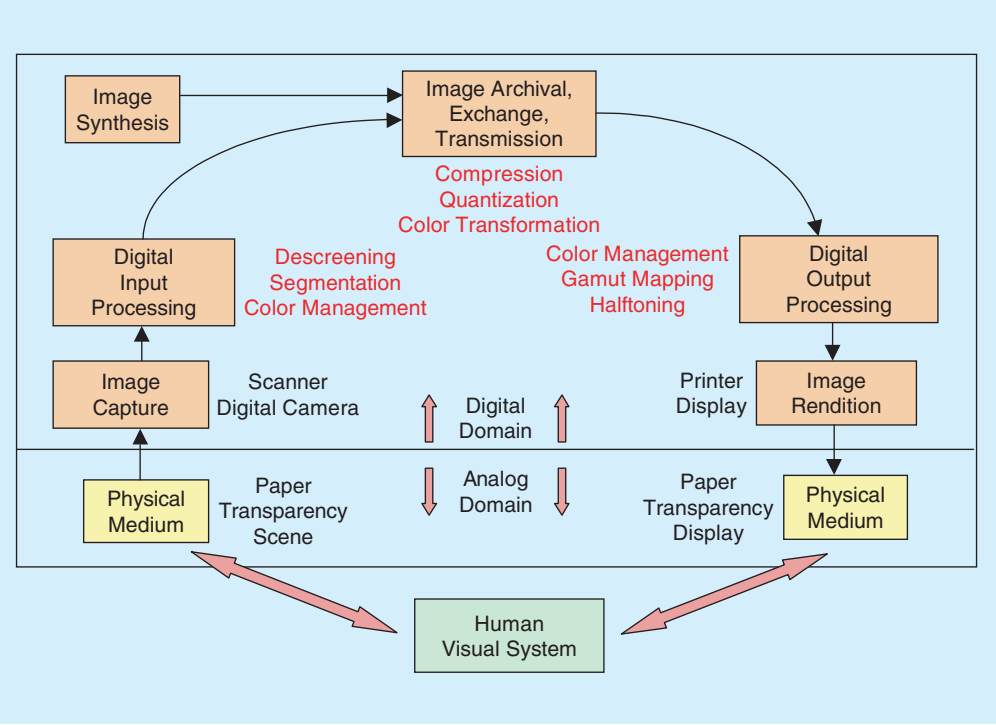

[FIG1] Overview of digital color imaging system. Digital imaging operations are listed in red text.

optimization opportunities offer the best tradeoffs and potential for improvement in today's digital color imaging devices.

EXAMPLES OF SYSTEM OPTIMIZATION IN DIGITAL COLOR IMAGING SYSTEMS

Recent literature in the digital color imaging area offers a number of approaches that illustrate the benefits of exploiting interactions among system elements in the optimization process. The following is a brief overview of some of these techniques. Two detailed examples are then presented.

A common theme in several of the approaches is the joint treatment of color and spatial dimensions, which are normally handled independently and separately. Consider the reproduction of JPEG-compressed color images on a printer. The standard workflow is to first perform decompression, followed by a printer characterization transform that maps the input image, typically in a device-independent color space such as YC_bC_r, to printer cyan, magenta, yellow, and black (CMYK). Klassen et al. [17] have developed a technique to combine the decompression and color characterization operations in a manner that significantly enhances computational performance. The basic idea is to parse the printer characterization transform into an expensive three-dimensional (3-D) correction and a simple one-dimensional (1-D) correction, and apply the former only to a small $N \times N$ subblock within each 8×8 image block ($N \ll 8$) in the discrete cosine transform domain afforded by the JPEG model. In a similar vein, McCleary [18] addresses the problem of noise introduced by color correction of digital camera images. Observing that these images are then subsequently JPEG compressed, he proposes a method to synergistically combine the color correction and JPEG compression in order to reduce the noise.

WE SHOW THAT OPTIMIZATION OF THE QUALITY AND PERFORMANCE OF A COLOR IMAGING SYSTEM IS INDEED A SYSTEM-WIDE PROBLEM THAT MUST TAKE INTO ACCOUNT INTERACTIONS AMONG THE VARIOUS COMPONENTS.

A problem commonly encountered in halftoning for CMYK printing is color moiré [19], [20], an objectionable low-frequency beat pattern resulting from the superposition of multiple high-frequency halftone screens. Traditional methods to combat color moiré involve carefully optimizing the halftone screen angles to minimize the visibility of the artifact. Balasubramanian and Eschbach [21] have observed that the moiré can also be reduced by adjusting the continuous tone signals driving the halftone screens. This adjustment occurs in the color characterization function executed prior to the halftoning step. Thus, moiré minimization is treated as an objective in the joint optimization of color characterization and halftoning.

For devices with limited color capabilities or limited memory for image display, it is common practice to quantize the colors to a smaller palette and then approximate the desired image using colors from the palette [14]. The former operation is typically referred to as color quantization, and the latter is a generalized halftoning step. The need for color quantization first arose in desktop displays with limited image memory for display. While these displays are now rare in desktop systems, there is renewed interest in color quantization for wireless devices whose displays are restricted in their size, memory, and power consumption [22]. While most work in color quantization treats the color quantization and halftoning steps independently and sequentially, the performance can be improved by jointly optimizing these operations. Puzicha et al. [23] have recently proposed an elegant solution to this problem. They formulate a visually motivated cost function that encapsulates the combined cost of palettization and of the assignment of pixels to the palette colors. Efficient algorithms based on multiscale deterministic annealing determine a spatially quantized image that optimizes the cost function. The results are a significant improvement over sequential processing, particularly for small thumbnails that are often necessary on mobile devices. Illustrative results from their technique may be found online [23]. The technique can also be applied to the case where the output images are binary halftones, for which its cost function becomes similar to that used for other model-based halftoning techniques [24]–[26], which themselves are examples of system optimization that explicitly incorporate the human observer instead of developing heuristic techniques based on HVS characteristics. Benefits from system optimization have also been realized in color output rendering for hardcopy through the use of techniques that consider printed color separations jointly rather than individually. Specifically, for clustered-dot halftoning schemes the use of nonorthogonal halftone screens [15], [24], [27] offers the capability for reduced moiré through suitable selections of a set of screens corresponding to the separations [15]. While a similar concept has been the basis of analog halftone screens for lithographic printing for a long time, the issue has only recently been addressed in the context of the rectilinear grids necessitated by digital halftoning. Robust system optimization techniques for this problem have also been proposed earlier in [19]. Similarly, for dispersed dot screens and error diffusion, joint considerations of color texture from overlap of multiple separations in print has yielded significant improvements with little additional computational cost [28], [29]. Some recent work in this field also incorporates considerations from misregistrations in halftoning/halftone design [30], [31] thereby addressing system wide robustness that goes even beyond the color imaging components.

Finally, we highlight one more example of joint spatial and color considerations applicable for scan to print applications involving halftone input and halftone reproduction. In such systems, the interaction between input and output halftones can generate objectionable rescreening moiré even though the input sampling satisfies the well understood Nyquist sampling criterion. Traditionally, this problem has been addressed by

descreening the scanned image prior to halftoning on the output side, a process that corresponds to a form of low-pass filtering (potentially nonlinear) and invariably leads to loss of high frequency detail. Novel approaches that do not suffer from this limitation have been proposed to address this problem in recent work [32], [33]. Instead of considering the spatial halftoning operation independently of the color, these techniques employ a combined spatial and color model of the output device. This model enables prediction of the output spatial image, which includes the halftone spatial structure and therefore also mimics the re-screening moiré. Low-pass differences between the predicted output image and the desired image represent the prediction of the moiré, which can be precompensated for in the input. The resulting algorithm may be understood in signal processing terms as a feedback compensation scheme as opposed to the heuristic low-pass filtering techniques.

In the following, we present in some detail two specific examples that illustrate how the interplay among system elements can be beneficially exploited in system optimization.

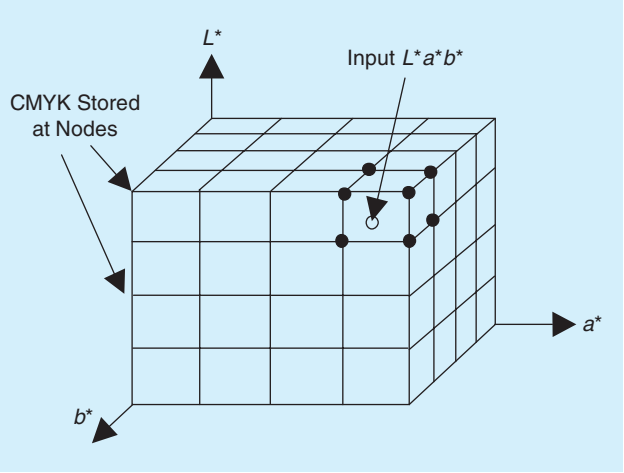

[FIG2] Example of a 3-D LUT transformation from CIELAB to CMYK. The open circle is the input point to be mapped, and the surrounding black circles are the points used for interpolation.

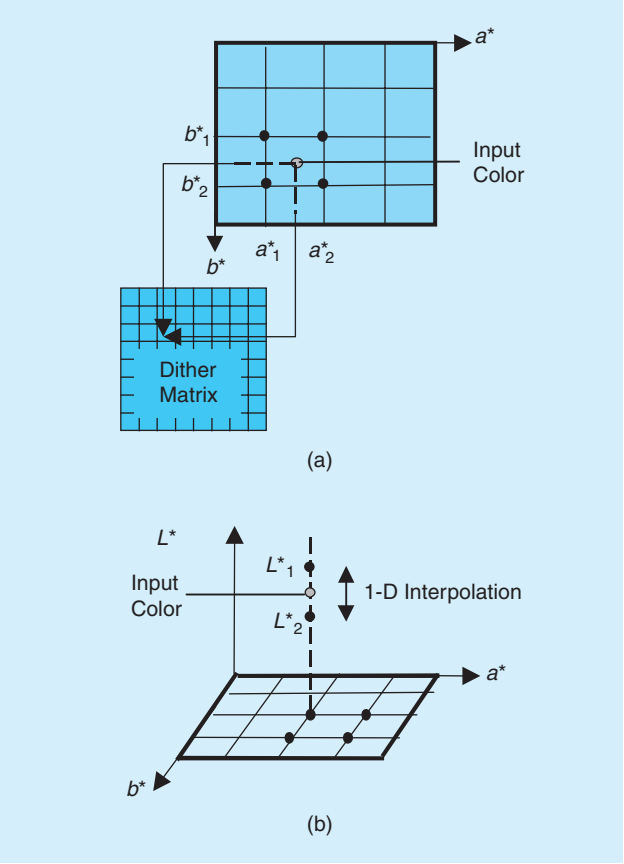

[FIG3] (a) Multilevel halftoning along the two chrominance (a*, b*) dimensions using a spatial dither matrix; (b) 1-D interpolation along luminance or lightness (L*).

LOW-COST COLOR LOOKUP TABLE TRANSFORMS EXPLOITING SPATIAL INTERACTIONS

A primary goal of color management in hardcopy imaging systems is to achieve consistent and accurate color reproduction across different devices. This necessitates the derivation and application of color correction transformations that correct for the nonlinear behavior of both the device and the HVS. The color transformations are typically complex multidimensional functions, which makes the real-time processing of image data a computationally prohibitive task. To reduce computational cost, the functions are typically implemented as multidimensional lookup tables (LUTs).

For hardware economy, the LUTs constitute a sparse sampling grid of nodes that partition the 3-D input color space into a set of rectangular cells. An example is shown in Figure 2 for a transformation from CIELAB to printer CMYK. Given an input color, the LUT transformation comprises two basic steps: 1) retrieval of a set of nodes lying on the enclosing rectangular cell and 2) 3-D interpolation among these nodes. LUTs are invariably built on a regular rectangular grid so that the cell retrieval step can be performed with minimal computation. Most of the computational cost thus lies in the interpolation step. Many interpolation schemes exist. In 3-D, these include trilinear, prism, pyramid, and tetrahedral interpolation [34]. Of these, tetrahedral interpolation requires the fewest computations, and all three require comparable storage and memory.

For some applications, the computational cost of 3-D interpolation can be prohibitive. Examples of such applications include very high-speed printing and rendering on devices with limited computational resources. It is beneficial in these instances to improve the performance of the LUT transformation, while yet maintaining acceptable output quality. A promising approach for reducing this cost is to apply multilevel halftoning among neighboring nodes of the LUT [35], [36]. For each input color, exactly one of the neighboring nodes in the enclosing cell is selected for output based on a spatial dither mask. The basic idea behind these approaches is that the halftoning introduces a high-spatial frequency pattern that is least noticed (effectively averaged) by the visual system. In other words, the intermediate levels normally obtained by interpolation are achieved via visual averaging of a high-spatial-frequency halftone pattern. This technique

exploits several interactions and dependencies. First, it recognizes that human color perception is a function of spatial dimensions, being far less sensitive to color variations at high spatial frequencies. Second, for binary output devices, the impact on visual quality can be minimized by exploiting the fact that the output signals from the LUT undergo subsequent binary halftoning. This is, therefore, another good example of exploiting system interactions to improve performance.

A variant of the aforementioned approach exploits the fact that the HVS is even less sensitive to high-frequency variations in chrominance than in luminance [37]. Assuming the input color space of the LUT transformation is a luminance-chrominance representation, multilevel halftoning is applied only in the two chrominance dimensions, while 1-D interpolation is applied in the luminance dimension. This is shown schematically in Figure 3. The dither matrix employed in this approach was the Bayer dispersed dot matrix [38], [37].

Figure 4 compares the output from standard 3-D tetrahedral interpolation with that of the proposed chrominance halftoning scheme. The input image was represented in CIELAB coordinates and was converted to CMYK for a Xerox 5795 laser printer. A $16 \times 16 \times 16$ LUT, with nodes uniformly distributed along each of the L*, a*, and b* axes was used to perform the conversion using either the standard or proposed LUT transformation techniques. The CMYK images were then converted to CIELAB using a printer model and then transformed to sRGB for inclusion in this document. Figure 4 is thus a soft proof of the printed output. (Note that reprinting of these images on an uncalibrated printer can produce additional errors and artifacts. The reader is encouraged to judge color quality of the electronic version of this article on a standard CRT with characteristics similar to sRGB.) The differences between the standard and proposed techniques manifest themselves mostly as high-frequency chrominance textures in the smooth background regions. Recall that the image actually undergoes an additional binary halftoning step before printing. This step, which cannot be effectively simulated in the soft proofs in Figure 4, often serves to mask the high-frequency textures introduced by the multilevel chrominance halftoning. Another observation is that from our experiments, the use of multilevel halftoning in all three dimensions of the LUT (as proposed by [35] and [36]) introduces textures in the luminance channel as well as chrominance. The luminance textures are more easily perceived by the HVS and more difficult to mask in the binary halftoning step. Finally, the textures can be reduced by simply increasing the size of the LUT along the dimensions in which multilevel halftoning is performed.

Table 1 compares the computational cost of standard interpolation techniques (tetrahedral and trilinear) with the proposed approach of chrominance halftoning in conjunction with 1-D luminance interpolation. It is evident that significant computational savings can be had with the proposed technique. The cost benefit comes from the fact that halftoning is far less computationally intensive than 3-D interpolation.

(a)

(b)

[FIG4] Images comparing (a) 3-D tetrahedral interpolation with (b) chrominance halftoning and 1-D luminance interpolation.

[TABLE 1] COST ANALYSIS COMPARING STANDARD AND PROPOSED LUT TRANSFORMATION TECHNIQUES. N IS THE NUMBER OF OUTPUT SIGNALS. M, A, C, AND S DENOTE MULTIPLICATIONS, ADDITIONS, COMPARISONS, AND SHIFT OPERATIONS, RESPECTIVELY. T DENOTES EXECUTION TIME IN μSEC TO PERFORM INTERPOLATION FOR EACH PIXEL ON A SUN SPARC20 WORKSTATION WITH A 75 Mhz CPU.

INTERPOLATION ALGORITHM	M	A	C	S	T (μs)
1) TRILINEAR	7N	7N+2	0	2	18.0
2) TETRAHEDRAL	3N	3N+2	2.5	2	12.0
3) PROPOSED METHOD	N	N+4	0	2	5.9
4) % SAVINGS FROM (2) TO (3)	67	43	100	0	51

COLOR CORRECTION EXPLOITING MEDIA CHARACTERISTICS

It is well known that the color characteristics of input and output devices are quite strongly dependent on the "medium" being captured or rendered to, respectively [39], [40, p. 290], [41], where medium refers to the combination of colorants and substrates for hardcopy prints and, more generally, to spectral characteristics of the input for capture devices such as digital cameras. For input devices, the problem can be minimized

through an optimized design of the capture device's spectral sensitivities. This is achieved by using a comprehensive system-wide metric that incorporates the impact of the end human observer, the statistical characteristics of the input, and the system noise [42]–[45]. However, such optimization is rare in current consumer image capture devices. In many systems, the characterization for input or output is optimized for only one medium and utilized for the multiple different media used in practice. This simplification occurs mainly because recharacterization for every new medium is time consuming and costly. For output devices, recent work [41] shows one can use an accurate characterization for a single reference medium and a minimal number of additional measurements to characterize the device for each new media. There still remains the challenge of associating, at the system level, the correct characterization profile for a given document based on the user's selection of medium. Using wider system knowledge, the problem for color scanners, in particular, can be mitigated. How this is done is highlighted in the following.

THESE SYSTEM OPTIMIZATION OPPORTUNITIES OFFER THE BEST TRADEOFFS AND POTENTIAL FOR IMPROVEMENT IN TODAY'S DIGITAL COLOR IMAGING DEVICES.

The spatial characteristics of the input can aid the selection of an appropriate color characterization profile for color scanners. The technique relies on the fact that typical inputs for these devices are themselves color hardcopy reproductions from other imaging systems. The images in Figure 5 depict scans from images printed with different printing technologies, captured at a resolution of 600 dpi. The scans correspond to small uniform regions in each print and are shown in a blown-up view here to illustrate the microstructure of the printed images. From the images, it is clear that their spatial structure identifies the printing technology. Since the photograph is a continuous tone process, its scan shows almost no spatial variation, while the scans from other technologies illustrate their halftone structure. Since halftoning techniques are typically matched to the printing technology for reasons of robustness and image quality [15], [46], the knowledge of the spatial characteristics may be exploited in order to classify the scanned input to the corresponding print technology, which in turn can be used to identify a color characterization profile (or group of profiles) for the input.

The principle of the technique is illustrated in Figure 6, where the estimated power spectra of the scanned images corresponding to the different marking technologies are shown. These images represent the two-dimensional power spectrograms [47] for the scanned images, where the dark regions represent concentrations of energy, and the color of each region indicates the concentration of energy in corresponding scanner color channels. The estimated power spectra clearly highlight the differences among the printing processes. The halftone technologies are all readily distinguished from the photograph by the much higher concentration of high frequency energy in the corresponding power spectra. Among the halftone technologies, the periodicity of halftones in lithographic and xerographic input images gives rise to sharp peaks in the power spectra at the locations of the halftone frequencies and their harmonics. These are therefore readily distinguished from the inkjet input where no peaks are observed in the power spectrum (other than the dc component) because the halftones are aperiodic. The periodic clustered halftones for lithographic and xerographic printing show considerable similarity

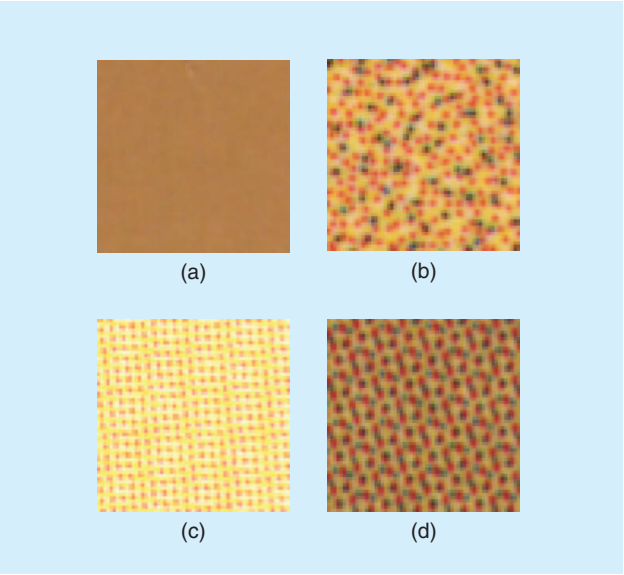

[FIG5] Scanned image regions from prints produced with different printing technologies: (a) photograph, (b) ink jet, (c) lithographic, and (d) xerographic.

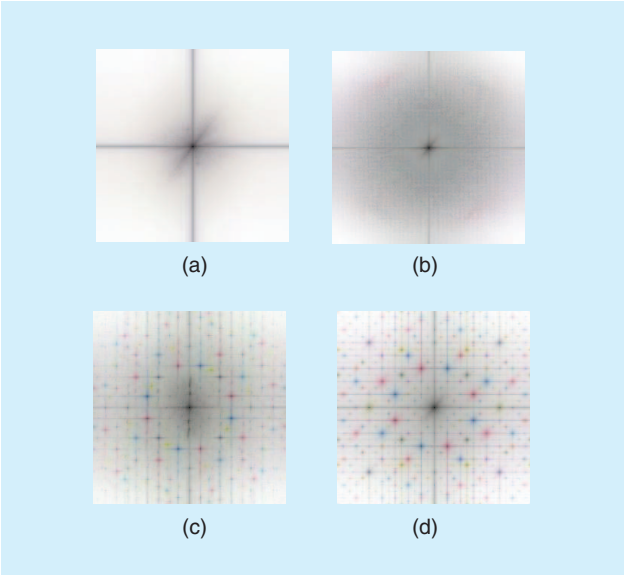

[FIG6] Two-dimensional power-spectra of scanned images produced with different printing technologies: (a) photograph, (b) ink jet, (c) lithographic, and (d) xerographic.

but can be distinguished based on the placement of the peaks in the power spectra and the noise characteristics. Additional details for the classification process can be found in [48], and computationally simpler techniques for the identification of the halftone process from the scanned data and comprehensive results are included in [49]. It is worth noting that spatial analysis of the input scanned image is often already conducted for the purposes of de-screening/ enhancement. Hence, the proposed scheme often does not entail significant additional computation in the overall system.

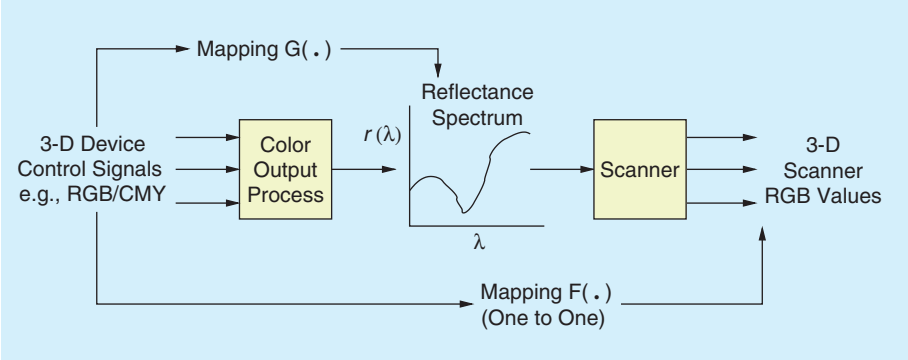

[FIG7] Block diagram illustrating the relationship between scanner RGB output, device signals used for creation of the input, and the reflectance spectra.

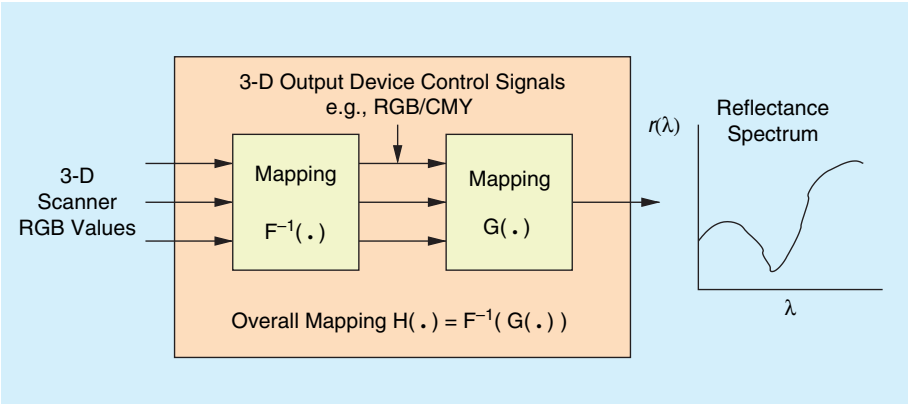

[FIG8] Spectrum recovery from scanner RGB values for color reproduction.

The aforementioned example illustrated how analysis of spatial characteristics of scanned images can be exploited for improving the accuracy of color characterization. In the example that follows, we illustrate that an exact knowledge of the input can often enable, not only a recovery of color, but also the complete spectral reflectance from scanner RGB values. Figure 7 illustrates the concept. The scanner senses the reflectance distribution at its input and reduces it to a 3-D RGB representation as illustrated in the rightmost two blocks of Figure 7. In the absence of additional information, the 3-D color information is clearly insufficient for accurately reconstructing the object spectral reflectance $r(\lambda)$. In most color scanning applications, however, the original input image that is to be electronically captured is itself a reproduction. This is the case, for instance, when a photographic print is to be scanned or a xerographically produced color document is to be copied. Since these reproductions are produced by exploiting the trichromacy of human vision, they are typically produced by using only three independent color controls as illustrated by the rightmost two blocks of Figure 7. Even for four color, CMYK printing devices (and other devices employing process colors), typically only three independent controls are exercised in practice, and the situation of Figure 7 applies.

If we consider the complete end-to-end system illustrated in Figure 7, under normal imaging conditions, the mapping $F(\cdot)$ from the 3-D device control signals used for printing to the corresponding scanner RGB values is one-to-one (ignoring quantization and noise artifacts). This one-to-one nature arises because the color production systems are designed to produce different colors in response to different input control signals, and even though scanners have confusion among scanned spectra, the confusion exists only among spectra for different media. The one-to-one nature of the mapping assures its invertibility, and, therefore, there exists a mapping $F^{-1}(\cdot)$ that can map the colorimetric values back to the 3-D device control signals that were used to produce the corresponding output. Figure 7 also illustrates the forward device response function $G(\cdot)$, which represents the mapping from 3-D device control values to the reflectance spectrum produced on the output device in response to those control values. A concatenation of the mappings $F^{-1}(\cdot)$ and $G(\cdot)$ thus allows scanner RGB values to be mapped to the corresponding spectral reflectance values for the given color production system. This is illustrated in Figure 8. Therefore, for the case where the input is known exactly, it is feasible to extract complete spectral reflectance data from scanner RGB data. A practical system for performing this spectral recovery in general situations is presented in [50]. The work uses a neural network to estimate the mapping $H(\cdot)$ and enables spectral reconstruction that has an error of under 1 ΔE^*_{94} units across multiple illuminants. We illustrate the technique in a more constrained setting, where a more direct signal processing solution is applicable. The method is based on set theoretic estimation [51] whose use has already been proposed for color problems [52].

For the case when the input is a photographic medium, the system is well approximated by the linear in spectral density model introduced in this issue [1]. Using the same notation, we note that the spectrum $\mathbf{g}$ for a given point on the photographic print illuminated by a light source $\mathbf{l}$ can be expressed in optical density domain as

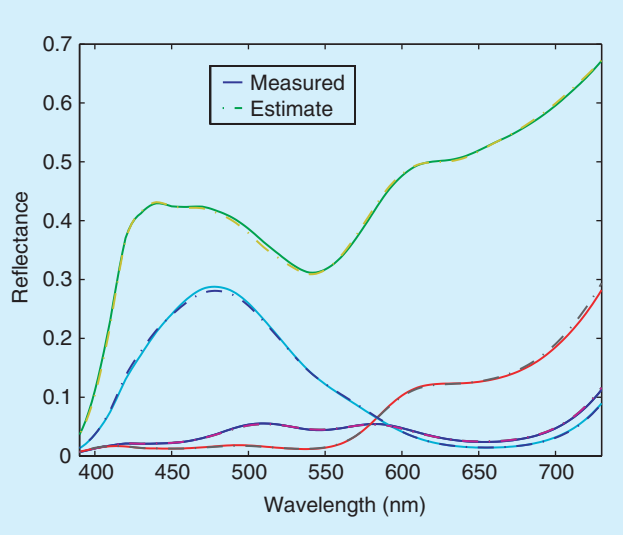

[FIG9] Representative results illustrating measured photographic reflectance spectra versus estimates from model-based scanner calibration.

$$-\log_{10}(\mathbf{g}) = -\log_{10}(\mathbf{l}) + \mathbf{D}.\mathbf{c} \tag{1}$$

where the logarithm is applied term-wise to the vectors. For our particular case, the matrix $\mathbf{D}$ contains the spectral density of the CMY colorants used in the photograph, and the vector $\mathbf{c}$ is the concentration of these colorants at the point in consideration. Thus, in density space, the input spectra for the scanner illustrated in Figure 7 lie on a 3-D affine manifold. By exploiting additional system information, as we illustrate in the following, one can obtain an entirely model-based solution.

If $\mathbf{M}$ is the matrix of scanner spectral sensitivities, the scanner response to the spectrum $\mathbf{g}$ is

$$\mathbf{v} = \mathbf{M}^{\mathrm{T}}\mathbf{g}. \tag{2}$$

Thus, knowledge of the scanner RGB values $\mathbf{v}$ constrains its spectrum by three linear equations in the domain of spectral reflectance. If this constraint is used jointly with the constraint imposed by the model for the photographic medium, the spectrum may be uniquely determined from the scanner RGB values $\mathbf{v}$. One challenge remaining, however, is a robust algorithm for solving these joint constraints. While both sets of constraints are linear (technically, the constraint in density space is affine), they lie in different domains and therefore cannot be solved using simple linear algebra or by conventional convex set theoretic estimation schemes that require constraints to be convex in the same domain. The problem can be simplified, however, by using a novel set theoretic estimation technique [53] that maps the problem into a product space. The technique provides not only a robust solution to the specific problem considered here, but also a general formulation [54] that is applicable to a wider set of problems in subtractive color.

The problem of estimating the spectra of photographic prints from scanner RGB data is reduced to a problem of joint satisfaction of convex closed constraints through an application of the results in [53] to the models of (1) and (2). The method of projections onto convex sets (POCS) therefore provides a robust technique for solving the problem. Of course, practical use of the algorithm also requires knowledge of the spectral density $\mathbf{D}$. For typical situations where this knowledge is not explicitly available, it may be estimated to within a nonsingular transform by using principal components analysis on a small number of measured density values from the photograph being scanned itself [54]. This allows one to have a targetless scheme for spectral calibration of scanners [55], wherein the spectral sensitivity of the scanner along with a few spectral measurements from the image being scanned allow the scanner to accurately estimate spectral data from the scanned RGB values. Illustrative results from this technique are presented in Figure 9, where four estimated spectral reflectances (shown as broken lines) are compared against the corresponding measured values (shown as solid lines). From these plots, it is apparent that the technique provides accurate estimates of the spectra. Over a typical photographic calibration target, the aforementioned technique provides accuracy of around 1.8 ΔE^*_{ab} units, which is quite comparable to other nonspectral calibration schemes [55]. The spectral calibration offers advantages over the conventional color calibration methods, in that the colorimetry under different viewing illuminants may be subsequently calculated, which is not possible if only a colorimetric calibration is available.

CONCLUSIONS

We have attempted to show, via several examples, that optimization of the quality and performance of a color imaging system is indeed a system-wide problem that must take into account interactions among the various components. In addition to the examples described earlier, other instances of color imaging system interactions can be conceived. We believe that, in general, a systems approach rooted in signal processing principles typically offers improved "operating points" in the computation and quality tradeoff "operating curves." In many cases, the systems approach can actually simplify the optimization of the individual components, as is illustrated by the example of joint optimization of device characterization and halftoning to minimize moiré [21]. In other cases, overall system performance is improved at no additional cost. Our second example illustrated this where the intelligent use of spatial side information obtained in the scanning process improved input color characterization accuracy. The article will hopefully provoke more engineers working on color imaging to also think in terms of systems and create additional examples of the benefits of such thinking.

AUTHORS

Raja Bala is a principal scientist in the Xerox Innovation Group, working on color imaging algorithms for Xerox's color products. He received a Ph.D. degrees from Purdue University in electrical

engineering. His Ph.D thesis was on efficient algorithms for color quantization of images. He is also an adjunct professor in the Electrical Engineering Department at the Rochester Institute of Technology. He holds more than 30 patents and more than 40 publications in the field of color imaging. He is a member of IS&T.

Gaurav Sharma is an associate professor in the Electrical and Computer Engineering Department and the Department of Biostatistics at the University of Rochester, New York. His research interests include color imaging, multimedia security, and bioinformatics. He received a Ph.D. in electrical computer engineering from North Carolina State University. He is a Senior Member of the IEEE and currently serves as an associate editor for *IEEE Transactions on Image Processing* and the *SPIE/IS&T Journal of Electronic Imaging*.

REFERENCES

[1] H.J. Trussell, M.J. Vrhel, and E. Saber, "Overview of the color image processing issue," *IEEE Signal Processing Mag.*, vol. 22, no. 1, pp. 14–22, 2005.

[2] G. Sharma, Ed., *Digital Color Imaging Handbook*. Boca Raton, FL: CRC, 2003.

[3] R. Ramnath, W.E. Snyder, Y.F. Foo, and M.S. Drew, "Color image processing," *IEEE Signal Processing Mag.*, vol. 22, no. 1, pp. 34–43, 2005.

[4] K. Parulski and K. Spaulding, "Color image processing for digital cameras," in *Digital Color Imaging Handbook*, G. Sharma, Ed., Boca Raton, FL: CRC, 2003, ch. 12.

[5] H.J. Trussell and R.E. Hartwig, "Mathematics for demosaicking," *IEEE Trans. Image Processing*, vol. 11, no. 4, pp. 485–492, Apr. 2002.

[6] D. Taubman, "Generalized Wiener reconstruction of images from colour sensor data using a scale invariant prior," in *Proc. Int. Conf. Image Processing*, vol. 3, 2000, pp. 801–804.

[7] R. Bala, "Device characterization," in *Digital Color Imaging Handbook*, G. Sharma, Ed. Boca Raton, FL: CRC, 2003, ch. 5.

[8] K.T. Knox, "Integrating cavity effect in scanners," in *Proc. IS&T/OSA Optics Imaging Information Age*, Rochester, NY, 20–24 Oct. 1996, pp. 83–86.

[9] J. Luo, R. de Queiroz, and Z. Fan, "A robust technique for image descreening based on wavelet decomposition," *IEEE Trans. Signal Processing*, vol. 46, no. 4, pp. 1179–1184, Apr. 1998.

[10] Z. Fan, "Unscreening using a hybrid filtering approach," in *Proc. IEEE 1996 Int. Conf. Image Processing*, Lausanne, Switzerland, Sept. 1996, pp. 351–354.

[11] Z. Xiong, M.T. Orchard, and K. Ramchandran, "Inverse halftoning using wavelets," *IEEE Trans. Image Processing*, vol. 8, pp. 1479–1482, Oct. 1999.

[12] J. Morovic, "Gamut mapping," in *Digital Color Imaging Handbook*, G. Sharma, Ed. Boca Raton, FL: CRC, 2003, ch. 10.

[13] R. deQueiroz, "Compression of color images," in *Digital Color Imaging Handbook*, G. Sharma, Ed. Boca Raton, FL: CRC, 2003, ch. 8.

[14] L. Brun and A. Tremeau, "Color quantization," in *Digital Color Imaging Handbook*, G. Sharma, Ed. Boca Raton, FL: CRC, 2003, ch. 9.

[15] C. Hains, S. Wang, and K.T. Knox, "Digital color halftones," in *Digital Color Imaging Handbook*, G. Sharma, Ed., Boca Raton, FL: CRC, 2003, ch. 6.

[16] E.J. Giorgianni and T.E. Madden, *Digital Color Management: Encoding Solutions*. Reading, MA: Addison Wesley, 1998.

[17] R.V. Klassen, R. Balasubramanian, and R. deQueiroz, "Color correcting JPEG compressed images," in *Proc. IS&T and SID's 5th Color Imaging Conf.*, 1997, pp. 83–87.

[18] B. McCleary, "Methods to reduce the amplication of random noise in the color processing of imager data," in *Proc. IS&T's PICS Conf.*, 2003, pp. 50–57.

[19] Isaac Amidror, *Theory of the Moiré Phenomenon*. Norwell, MA: Kluwer, 2000.

[20] P.A. Delabatista "Screening techniques, moiré in four color printing," in *Proc. TAGA*, 1992, pp. 44–65.

[21] R. Balasubramanian and R. Eschbach, "Reducing multi-separation color moiré via a variable undercolor removal and gray-component replacement strategy," *J. Imaging Sci. Technol.*, vol. 45, no. 2, pp. 152–160, Mar./Apr. 2001.

[22] J. Luo, A. Singhal, G. Braun, R.T. Gray, O. Seignol, and N. Touchard, "Displaying images on mobile devices: Capabilities, issues, and solutions," in *Proc. 2002 IEEE Int. Conf. Image Processing*, pp. I-13–I-16.

[23] J. Puzicha, M. Held, J.M. Buhmann, and D.W. Fellner, "On spatial quantization of color images," *IEEE Trans. Image Processing*, vol. 9, no. 4, pp. 666–682, Apr. 2000.

[24] A.U Agar, F.A Baqai, and J.P. Allebach, "Human visual model-based color halftoning," in *Digital Color Imaging Handbook,* G. Sharma, Ed. Boca Raton, FL: CRC, 2003, ch. 7.

[25] T.N. Pappas and D.L. Neuhoff, "Least-squares model-based halftoning," *IEEE Trans. Image Processing*, vol. 8, no. 8, pp. 1102–1116, Aug. 1999.

[26] J.B. Mulligan and A.J. Ahumada, Jr., "Principled halftoning based on human vision models," in *Proc. SPIE/SPSE Conf. Human Vision, Visual Processing, Visual Display III*, vol. 1666, 1992, pp. 109–121.

[27] J.P. Allebach and F.A. Baqai, "Computer-aided design of clustered-dot color screens based on a human visual system model," *Proc. IEEE*, vol. 90, no. 1, pp. 104–122, Jan. 2002.

[28] Z. Fan and S. Harrington, "Improved quantization methods in color error diffusion," *J. Electron. Imaging*, vol. 8, pp. 430–437, Oct. 1999.

[29] S.J. Harrington, "Color images having multiple separations with minimally overlapping halftone dots and reduced interpixel contrast," U.S. Patent 5 631 748, May 20, 1997.

[30] Z. Fan, G. Sharma, and Shen-ge Wang, "Error-diffusion robust to mis-registration in multi-pass printing," in *Proc. PICS,* 2003, pp. 376–380.

[31] G. Sharma, Shen-ge Wang, and Z. Fan, "Stochastic screens robust to misregistration in multipass printing," in *Proc. SPIE,* vol. 5293, 2004, pp. 460–468.

[32] S. Wang and Z. Fan, "Moiré-free color halftoning using 2×2 printer modeling," in *Proc. SPIE,* vol. 4300, 2001, pp. 397–403.

[33] R. Levien, "Moiré suppression screening," in *Proc. SPIE*, vol. 3963, 2000, pp. 402–407.

[34] R. Bala and R.V. Klassen, "Efficient color transformation implementation," in *Digital Color Imaging Handbook*, G. Sharma, Ed. Boca Raton, FL: CRC, 2003, ch. 11.

[35] K.E. Spaulding and K.C. Scott, "Method and apparatus employing mean preserving spatial modulation for transforming a digital color image signal," U.S. Patent 5 377 041, Dec. 27, 1994.

[36] S.F. Weed and T.J. Cholewo, "Color space binary dither interpolation," in *Proc. IS&T and SID's 10th Color Imaging Conf.*, 2002, pp. 183–189.

[37] R. Balasubramanian, "Reducing the cost of lookup table based color transfomations," *J. Imaging Sci. Technol.*, vol. 44, no. 4, pp. 321–327, 2000.

[38] B.E. Bayer, "An optimum method for two-level rendition of continuous-tone pictures," in *Proc. IEEE 1973 Int. Conf. Commun.*, vol. 1, pp. 26.11–26-15.

[39] P.C. Hung, "Colorimetric calibration for scanners and media," *Proc. SPIE*, vol. 1448, pp. 164–174, 1991.

[40] H. Kang, *Color Technology for Electronic Imaging Devices.* Bellingham, WA: SPIE, 1997.

[41] M. Shaw, G. Sharma, R. Bala, and E. Dalal, "Minimal effort characterization of color printers for additional substrates," in *Proc. IS&T SID's 10th Color Imaging Conf.*, 2002, pp. 202–207.

[42] M. Wolski, C.A. Bouman, J.P. Allebach, and E. Walowit, "Optimization of sensor response functions for colorimetry of reflective and emissive objects," in *Proc. IEEE Int. Conf. Image Processing,* 1995, pp. II323–II326.

[43] G. Sharma and H.J. Trussell, "Figures of merit for color scanners," *IEEE Trans. Image Processing*, vol. 6, no. 7, Jul. 1997, pp. 990–1001.

[44] G. Sharma, H.J. Trussell, and M.J. Vrhel, "Optimal non-negative color scanning filters," *IEEE Trans. Image Processing*, vol. 7, no. 1, pp. 129–133, Jan. 1998.

[45] S. Quan, N. Ohta, M. Rosen, and Naoya Katoh, "Fabrication tolerance and optimal design of spectral sensitivities for color imaging devices," PICS 2001, pp. 277–282.

[46] H.R. Kang. *Digital Color Halftoning*. Bellingham, WA: SPIE, 1999.

[47] J.S. Lim, *Two-Dimensional Signal and Image Processing*. Englewood Cliffs, NJ: Prentice-Hall, 1990.

[48] G. Sharma, "Methods and apparatus for identifying marking process and modifying image date based on image spatial characteristics," US Patent 6 353 675, Mar. 05, 2002.

[49] G. Unal, G. Sharma, and R. Eschbach, "Efficient classification of scanned media using spatial statistics," in *Proc IEEE Int. Conf. Image Processing,* 2004, pp. 2395–2398.

[50] G. Sharma and S. Wang, "Spectrum recovery from colorimetric data for color reproductions," in *Proc. SPIE*, vol. 4663, 2003, pp. 8–14.

[51] P.L. Combettes, "The foundation of set theoretic estimation," *Proc. IEEE*, vol. 82, no. 2, pp. 182–208, Feb. 1993.

[52] H.J. Trussell, "Applications of set theoretic methods to color systems," *Color Res. Applicat.*, vol. 16, no. 1, pp. 31–41, Feb. 1991.

[53] P.L. Combettes, "Generalized convex set theoretic image recovery," in *Proc. IEEE ICIP,* 1996, pp. 453–456.

[54] G. Sharma, "Set theoretic estimation for problems in subtractive color," *Color Res. Applicat.*, vol. 25, no. 4, pp. 333–348, Oct. 2000.

[55] G. Sharma, "Target-less scanner color calibration," *J. Imaging Sci. and Tech.*, vol. 44, no. 4, pp. 301–307, Jul./Aug. 2000.

SP